ELECTRON CYCLOTRON RESONANCES IN ELECTRON CLOUD DYNAMICS *

C. M. Celata[a], Miguel A. Furman, J.-L. Vay, and Jennifer W. Yu[b], Lawrence Berkeley National Laboratory, Berkeley, CA 94720, U.S.A.

Abstract

We report a previously unknown resonance for electron cloud dynamics. The 2D simulation code "POSINST" was used to study the electron cloud buildup at different z positions in the International Linear Collider positron damping ring wiggler. An electron equilibrium density enhancement of up to a factor of 3 was found at magnetic field values for which the bunch frequency is an integral multiple of the electron cyclotron frequency. At low magnetic fields the effects of the resonance are prominent, but when B exceeds $\sim (2\pi m_e c/(e l_b))$, with l_b = bunch length, effects of the resonance disappear. Thus short bunches and low B fields are required for observing the effect. The reason for the B field dependence, an explanation of the dynamics, and the results of the 2D simulations and of a single-particle tracking code used to elucidate details of the dynamics are discussed.

INTRODUCTION

Electron cloud effects are an important consideration in modern colliders and storage rings and in other applications of intense positive beams such as heavy-ion-driven inertial fusion. As one example, because of intense synchrotron radiation from the beam, electron cloud effects are an essential factor in determining the positron damping ring design for the International Linear Collider (ILC). We have simulated the buildup of the electron cloud in this damping ring in the wiggler section using the 2D computer code POSINST [1]. Each simulation represented one x-y slice of the wiggler, and the field in that slice was taken to be that of an ideal dipole (constant uniform vertical field). The density distribution of the beam was assumed to be gaussian in all three dimensions, and it was not allowed to evolve, an assumption that is good on the timescale (a few microseconds) of the buildup.

Results of the simulation showed no dependence of the equilibrium average density of the cloud (i.e., the average density in the vacuum chamber after the cloud has built to its equilibrium value) on the dipole field strength, B, for fields above ~ 0.6 T. Below this field, however, the equilibrium density was enhanced by factors of up to 3 in very narrow (~ 10 G) field ranges. The reasons for these peaks in density and an explanation of the dynamics are given below.

SIMULATION PARAMETERS & RESULTS

The parameters used for our simulations were those of the ILC positron damping ring wiggler design. Beam parameters were: 2×10^{10} 5-GeV positrons per bunch; 6.15 ns bunch spacing; beam rms radii of 112 μm (σ_x), 4.6 μm (σ_x), and 6 mm (σ_z). The circular vacuum chamber radius was 2.3 cm, with a 1-cm (full height) antechamber at the midplane on the +x side. This is an unrealistic design for the ILC wiggler chamber, which would have an antechamber on both sides, but was originally used for this project because it began as dipole benchmarking runs. The detailed antechamber design does not qualitatively affect the results presented here. The number of synchrotron radiation photons hitting the wall was assumed to be 0.07 per e$^+$ per meter, with reflectivity of 1.0, so the photons were deposited uniformly along the wall surface except at the antechamber (no photons). Since this produces electrons at all x (except in a small region near the antechamber), using this uniform reflectivity allowed us to observe electron dynamics everywhere, even though electrons are tied to field lines except near the beam. The quantum efficiency of photoelectron production was assumed to be 0.1. The secondary emission model of Furman and Pivi [2] was used, with a peak secondary yield at normal incidence of 1.4 at 195 eV. Coefficients needed by the model were obtained by extrapolation from CERN Super Proton Synchrotron data for a stainless steel surface (see ref. 2). An integration time step of 1.25×10^{-11} and spatial grid size for the particle-in-cell grid (used for calculating electron dynamics) of 0.36 mm were found to be adequate for accurate results.

As mentioned above, the results of the simulations showed peaks in the equilibrium average density at low B. We have identified the fields at the peaks as those at which the ratio of the cyclotron frequency to the bunch frequency, n, is an integer. Since at these low fields the time for the bunch to pass is much less than the cyclotron period, when a bunch passes electrons get a nearly instantaneous kick that rotates their $v_\perp$ toward a direction parallel to the beam kick. When n is an integer, each time a new bunch passes the electron is at the same location, and the $v_\perp$ receives reinforcing kicks—i.e., there is a cyclotron resonance. Resonance will take place where

$$B = n \frac{2\pi m_e}{e \tau_b}, \qquad (1)$$

where τ_b is the bunch spacing, m_e is the electron mass,

[a] Also a visitor at California Institute of Technology
[b] Presently a student at Cornell University, Ithaca, NY, USA

and e is its charge. Since the field is spatially uniform, all electrons will be in resonance when Eq. (1) is satisfied. Fig. 1 shows the equilibrium average density resulting from each of 330 simulations graphed vs. n. Each peak falls on an integral value of n. Though runs were not done to outline every peak, for B<0.6 T any simulation done at integral n produced a peak.

Figure 2 shows the spatial distribution of electrons in the chamber, averaged over the simulation time period, for a resonant and a non-resonant case. Since for most of the simulation the density is at its equilibrium value, that time period is well represented by the figure. It is clear that the "stripes" pattern, with electrons confined to very narrow bands near the beam, that is seen at fields with no resonance is changed radically in the resonance case. At resonance the peak density in the chamber is lower, but since the spatial distribution is much broader a higher average density is obtained. This change in the spatial distribution is important when choosing the location of electron cloud diagnostics on the chamber wall. It also indicates that at resonant fields the distribution of wall heating and effects of the electron cloud on the beam are likely to be very different from those at non-resonant fields.
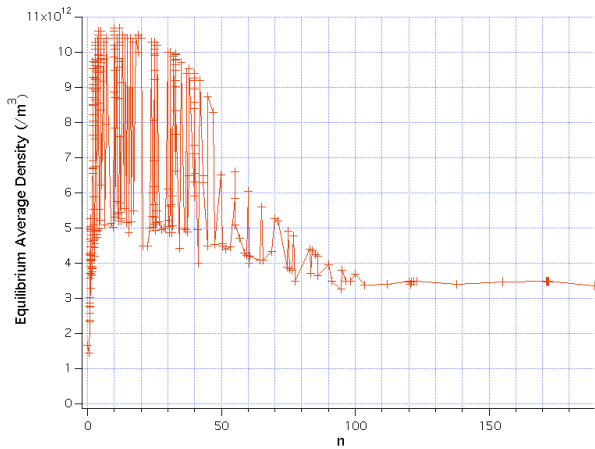

Fig. 1 Equilibrium average density vs. n. Simulations were done only at plus sign markers, which have been connected by lines to guide the eye.
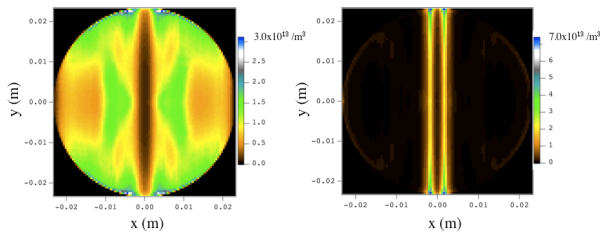

Fig. 2 Density distribution for 0.07 T (n=12) and 0.8 T (n=137.8). The circular vacuum chamber fits exactly within the plot boundaries.

A single particle tracking code was written to elucidate the dynamics of electrons, with the simplifying assumption that electron space charge was neglected. In the POSINT simulations the effects of space charge are

evident starting at about 0.15 μs. For the tracking code the force of the beam on the electrons was assumed to be an instantaneous kick. The tracking code confirmed that the beam kick quickly rotates the perpendicular electron velocity to a direction close to parallel to the x axis, and thereafter each bunch passage increases the magnitude of the perpendicular momentum. This increases the electron energy, and, by increasing $v_\perp$ but not v_{ll} over what is found in the non-resonance case, also causes the impact angle of the electron when it strikes the vacuum wall to be farther from the normal. Both of these effects increase the effective secondary electron yield (SEY). Detuning from resonance due to an increase in the relativistic mass could also be seen, but almost all electrons in the POSINST simulations hit the wall while this effect is still negligible.

Results from POSINST confirm the single particle results, producing similar energy spectra. Simulations also show the expected increase in $v_\perp$ at resonance, no obvious change in $v_{||}$, and a decrease in the cosine of the impact angle (see Fig. 3). The increase in $v_\perp$ occurs at all x, which is consistent with Fig. 2.
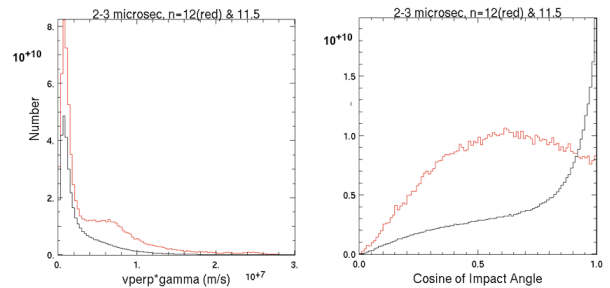

Fig. 3 Histograms for n=11.5 (black) and n=12 (red) for electrons hitting the wall from 2 to 3 μs after beam injection (i.e., after the cloud has reached equilibrium). Number of electrons vs. $\gamma v_\perp$ (left) and cosine of impact angle measured from the normal to the wall (right) are shown.

As seen in Fig. 1, the magnitude of the density peaks decreases as B increases, until for n greater than about 100 there is no longer a dependency of the cloud density on B. In the explanation of the resonance given above, we have assumed that the beam gives an instantaneous kick to the electron, and since the bunch spacing is an integral number of cyclotron periods, the electron is at the same position in its orbit the next time a bunch arrives. However as the magnetic field increases the cyclotron period becomes comparable to the time it takes for the bunch to pass an electron. Then the concept of resonance just described breaks down. The force of the beam is averaged over the cyclotron phase, leading to a negligible effect. The peaks will thus appear when

$$B << 2\pi \frac{m_e c}{e l_b}, \qquad (2)$$

where l_b is the bunch length. Thus the resonance effect on the density would appear for short bunches in regions of

low magnetic field, i.e., wigglers near the field minima or magnet fringe fields. This is likely to be why, to our knowledge, this effect has not been discussed before in the electron cloud literature, since most studies have been done for longer bunches and higher fields.

Finally, there are features of the density vs. B curve at low B that can be seen in the expanded view of Fig. 4. Double peaks are evident, with the central minimum gradually disappearing with increasing B. It becomes negligible at about n=12. From an examination of the simulation data for n=2 and n=1.93 (the peak below n=2) it appears that the reason for this is that electrons at, and very close to, the resonance stay in the system longer, acquiring higher energy than those at the nearby density peak. Though their energy is not too high to productively produce secondaries, their longevity means that the rate of electrons hitting the wall is lower than for n=1.93, so fewer secondaries are produced. This is confirmed by energy and $v_\perp$ spectra and by the fact that the average SEY is very similar for the two simulations, while the average wall bombardment rate is 23% lower at n=2 than at n=1.93. It should be noted that the densities for the two cases do not become significantly different from each other until after space charge becomes a significant effect. Therefore any further explanation of this double-peak phenomenon is likely to need to take electron space charge into effect.
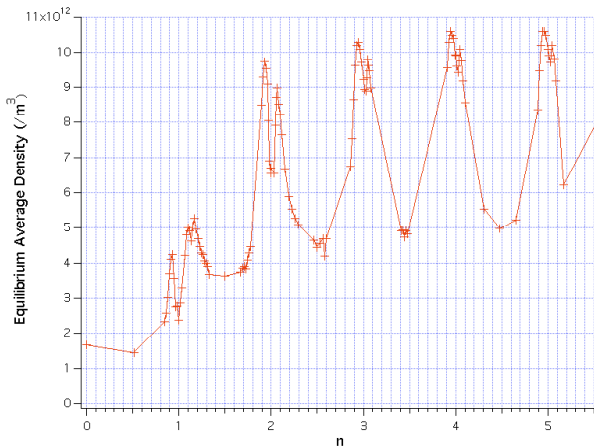

Fig. 4 Double peaks at low B.

The decreasing peak density as n decreases from 4 to 1 appears to be due to finite gyroradius effects. Comparing simulations at n=1 and n=2 we see many more electrons with energies above 100 eV (gyroradius for 100 eV at n=1 is 0.58 cm, and 0.29 cm for n=2) in the n=2 case, and the average energy of electrons hitting the wall is 118 eV for n=1 and 180 eV for n=2, indicating that the higher energy electrons are being lost in the n=1 case. Electrons with the same $v_\perp$ for the two cases also, on average, remain in the simulation longer in the n=2 case. As further evidence, simulation energy spectra show many more high-energy electrons hitting the wall for n=2 than for n=12, though there are more higher energy electrons confined in the chamber in the n=12 case.

The cyclotron motion of an electron in the presence of the periodic force produced by the beam is a driven harmonic oscillator problem. We have solved the corresponding single-particle equations under certain simplifying assumptions (driving force independent of electron location, electrons remain nonrelativistic, wall impacts ignored, radius of the gyro motion small compared to the vacuum chamber dimensions). The analysis, which will soon be submitted for publication, shows the expected growth in transverse energy when the resonant condition n=integer is satisfied, and reveals an exponential factor $(\exp(-(\omega_c \tau_b)^2/2)$, where ω_c=cyclotron frequency, τ_b=RMS bunch duration) which, in agreement with the explanation given above, accounts for the disappearance of the density peaks at high B and/or long bunches.

Experimental evidence of these effects has been observed (see paper MOPP063 at this conference by Pivi et. al.) with a retarding field analyzer (RFA) at the electron cloud experiment chicane at PEP-II when the dipole field there was varied [3]. The measured electron flux shows resonance peaks and valleys with the predicted spacing as the dipole field is ramped, but the locations of the peaks are systematically shifted from the predicted values. This shift, along with other details in the data, may be due to 3D effects and/or geometrical details of the RFA not yet included in our simulations, and are the subject of intense scrutiny at present.

COMMENTS & FUTURE WORK

The resonance effects discussed in this report are relevant for short bunches and low magnetic field regions, such as might be found in wigglers or magnet fringe fields. While the resonant density enhancement is not extremely large, it can have a certain periodicity in an accelerator (that of the dipoles, or of the wiggler period) that could cause resonances with beam motion. It will be important to redo this study with a 3D simulation, since the ExB drift can move electrons in the z direction, taking some electrons out of resonance and sending others into resonant fields. Whether this increases or decreases the density remains to be discovered. It will also be important to do the calculations with a realistic magnetic field profile, which will have some variation across the cross section, therefore decreasing the effect.

REFERENCES

[1] M. A. Furman and G. R. Lambertson, Proc. MBI-97, KEK Proc. 97-17, Dec. 1997 (Y. H. Chin, ed.), p. 170. M. A. Furman, LBNL-41482/CBP Note 247/LHC Project Report 180, May 20, 1998.
[2] M.A. Furman and M.T.F. Pivi, PRST-AB **5**, 124404 (2002).
[3] Private communication, Mauro Pivi and Johnny Ng.